International Journal of Nanoelectronics and Materials
IJNeaM
ISSN 1985-5761 | E-ISSN 2232-1535

Antibacterial activity of ZnO nanomaterials against *E. coli* using bioreductors from pineapple extract

Tengku Emrinaldi[a], Iwantono Iwantono [a] *, Febrina Wulandari[a], Yuda Arya Baskara[a], Arif Darma Saputra[a], Mayta Novaliza Isda[b], Puji Nurrahmawati[c], Suratun Nafisah[d], Romi Fadli Syahputra[e], Marlia Morsin[f]

[a]*Department of Physics, Faculty of Mathematics and Natural Science, Universitas Riau, Pekanbaru 28293 ,Indonesia*
[b]*Department of Biology, Faculty of Mathematics and Science, Universitas Riau, Pekanbaru 28293, Indonesia*
[c]*Department of Electrical Engineering, Faculty of Engineering, Universitas Negeri Padang, Padang 25132, Indonesia*
[d]*Department of Electrical Engineering, Institute Technology of Sumatera (ITERA) Way Hui, South Lampung 35365, Indonesia*
[e]*Department of Physics, Universitas Muhammadiyah Riau, Pekanbaru 28294, Indonesia*
[f]*Microelectronic and Nanotechnology – Shamsuddin Research Centre (MiNT-SRC), Institute of Integrated Engineering, Universiti Tun Hussein Onn Malaysia, Johor 86400, Malaysia*
* *Corresponding author. Tel.: +62-761-63273; fax: +62-761-63279; e-mail: iwantono@lecturer.unri.ac.id*

Received 25 June 2025, Revised 7 October 2025, Accepted 20 January 2026

ABSTRACT

Biosynthesis is a form of synthesis that involves the utilization of living organisms as biological agents. Zinc oxide is a versatile semiconductor material that exhibits antibacterial properties, thereby impeding the proliferation of germs. The objective of this research was to examine the impact of synthesis temperature on the properties of ZnO for its potential use as an antibacterial agent against E. coli. Zinc oxide (ZnO) nanomaterial powder was synthesized by a biosynthetic approach employing a combination of zinc nitrate hexahydrate (ZNH) and pineapple fruit extract. The synthesis temperature was varied at four different levels: 28°C, 50°C, 75°C, and 100°C. The physical properties of zinc oxide (ZnO) nanoparticles were examined using UV-Vis spectroscopy, X-ray diffraction (XRD), and field emission scanning electron microscopy (FESEM). The antibacterial activity was assessed using the disc diffusion method. This study provides empirical evidence supporting the efficacy of ZnO nanoparticles as antibacterial agents.

Keywords: *Antibacterial, Bioreductors, Biosynthesis, E. coli, Pineapple extract, Synthesis temperature, ZnO nanomaterials*

1. INTRODUCTION

Nanomaterials play a crucial role in the advancement of scientific and technological fields. There are two primary aspects that distinguish nanomaterials from bulk materials. First, nanomaterials possess a significantly smaller size, resulting in a larger surface-area-to-volume ratio. Second, nanomaterials exhibit particle sizes that fall within the nanoscale range[1]. Nanomaterials have versatile applications in diverse fields, including health[2], the environment, agriculture, food, industry, electrical equipment, and energy[1]. The antibacterial properties of ZnO nanomaterials have been observed to effectively impede the growth of many bacteria, including Salmonella enteritidis, Escherichia coli, Botrytis cinerea, and Penicillium expans*um*[3–5].

Zinc oxide (ZnO) is a white powder that exhibits limited solubility in neutral solutions but can dissolve in highly acidic or alkaline environments[6,7]. Additionally, it possesses favorable thermal stability[7–9]. ZnO has a band-gap energy of around 3.3 eV[10], rendering it highly suitable for application as an antibacterial agent[7]. At present, researchers have devised a novel approach to the synthesis of nanomaterials, known as the biosynthetic method, which entails the utilization of biological substances or microorganisms[8,11]. The biosynthetic process presents itself as a viable alternative because it uses environmentally sustainable ingredients, is easily accessible, is cost-effective, and avoids hazardous chemicals[12].

The purpose of this research is to utilize a biosynthetic method for the fabrication of ZnO nanoparticles and to evaluate their potential as antibacterial agents. The existing research gap lies in the limited systematic investigation of how variations in synthesis temperature influence particle formation, size, morphology, and antibacterial performance of ZnO nanoparticles produced from pineapple extract. Furthermore, a comparative analysis was conducted between these synthesized nanomaterials and commercially available ZnO. The ZnO samples were manufactured under controlled temperature conditions. Different synthesis temperatures can yield diverse types and sizes of nanomaterials[13–16]. The biological agents utilized in this study consisted of extracts derived from pineapples. Pineapple is known to possess various beneficial components, including vitamin C, phenolic compounds, and bromelain enzymes, which are associated with antimicrobial properties. The present study employed UV-Vis, XRD, and FESEM techniques for characterization, along with the disc diffusion method to assess antibacterial activity.

2. MATERIALS AND METHODS

2.1. Materials and Reagents

The materials utilized in this study encompassed pineapple (Ananas comosus), Zinc Nitrate Hexahydrate ($Zn(NO_3)_2 \cdot 6H_2O$), Sodium Hydroxide (NaOH), methanol, distilled water, Nutrient Agar (NA), Nutrient Broth (NB), Mueller Hinton Agar (MHA), Escherichia coli bacteria, 0.9% physiological NaCl, commercial ZnO, and disc paper with a diameter of 6 mm. All chemical reagents were purchased online from Sigma-Aldrich and Merck. The *Escherichia coli* culture was obtained from the Biology Laboratory of Riau University, while the distilled water used in the synthesis process was supplied by the Chemistry Laboratory of Riau University.

2.2. Preparation of Pineapple Extract

The extract sample originated from a recently harvested pineapple. The pineapple fruit was washed using distilled water, followed by the removal of its outer skin. Next, approximately 250 g of thoroughly cleaned pineapple was prepared for the extraction process. The juice of the pineapple fruit was extracted by squeezing and then filtered using Whatman paper. Ultimately, a total volume of approximately 60 mL of filtrate was obtained and then stored at a temperature of 10°C. This temperature was not intended as a negative condition, but rather to reduce enzymatic activity, prevent natural fermentation, and preserve the stability of bioactive compounds in the pineapple extract prior to its use in the ZnO synthesis process.

2.3. Biosynthesis of ZnO Nanomaterials

ZnO nanoparticles were synthesized via a biochemical pathway, namely biosynthesis. A solution containing 0.05 M ZNH and a solution containing 1 M NaOH were both diluted in 100 mL of distilled water. Subsequently, the solutions were transferred into a beaker and stirred using a magnetic stirrer until homogeneity was achieved. Zinc oxide nanoparticles were created through a chemical reaction between ZNH and 20 mL of pineapple extract, which was employed as a reducing agent. NaOH solution was used as an acidity regulator. A 1 M NaOH solution was incrementally added until the pH level reached 12. Temperature variations were applied during the nanomaterial growth stage by heating the biosynthesized solution in an oven at 28°C, 50°C, 75°C, and 100°C. Each temperature-treated sample was designated as ZAP (Zinc-Reducing Agent Product), referring to the ZnO produced under specific reducing-agent conditions. After the heating process, the samples were allowed to stand until precipitation occurred. The resulting precipitates were then separated, dried, and ground into a fine powder, which was subsequently characterized to determine their structural and morphological properties. The ZAP sample synthesized at the optimal temperature, yielding the highest-quality ZnO nanomaterials, was selected for further antibacterial activity testing[17–19].

2.4. Characterization and Antibacterial Test

In this study, a UV-1800 Shimadzu spectrophotometer with UV-Probe software was used to monitor the optical properties of the samples. X-ray diffraction (XRD) was performed using PANalytical equipment (Bruker, Netherlands), and the field emission scanning electron microscope (FESEM) used was the JEOL JSM-7600F Schottky series, manufactured in Japan. In addition, antibacterial assessment was conducted using the disc diffusion technique against Escherichia coli bacteria.

3. RESULTS AND DISCUSSION

3.1. XRD Analysis

Figure 1 displays the XRD patterns of ZnO nanomaterial samples and the reducing-agent-derived ZnO (ZAP). The ZnO crystal exhibits a total of nine diffraction peaks. The three largest peaks are observed at angles of $2\theta = 31.801°$, 34.479°, and 36.245°, corresponding to the crystal planes 100, 002, and 101, respectively. The observed diffraction pattern is consistent with the established diffraction pattern of ZnO material, as defined by Joint Committee on Powder Diffraction Standard (JCPDS) number 01-079-0205. The lattice parameters of pristine ZnO are a = 3.2069 Å and c = 5.1380 Å, which are in line with previous works[20]. Meanwhile, the ZAP samples under different synthesis temperatures show slightly higher values than pristine ZnO, as depicted in Table 1. This observed pattern provides evidence that the ZnO compound exhibits a crystalline structure known as wurtzite -hexagonal[21,22].

The crystal-size values of the ZnO and ZAP 28°C samples were determined using XRD characterization and data analysis employing the Scherrer equation[23,24]. The crystallite sizes of pristine ZnO and ZAP ranged from 23.95 nm to 27.14 nm. The average crystal size among these samples was determined to be 25.84 nm. The average crystal size is directly proportional to the resulting full width at half maximum (FWHM) value[25]. The large crystal dimensions suggest that the resulting spectrum becomes increasingly sharp and narrower [26].

Table 1. Lattice parameters of pristine ZnO and ZAP samples

Sample	a (Å)	c (Å)	c/a	D (nm)
ZnO	3.2069	5.1380	1.6022	23.95
ZAP 28°C	3.2507	5.2105	1.6029	26.44
ZAP 50°C	3.2490	5.2059	1.6023	25.58
ZAP 75°C	3.2444	5.1986	1.6023	26.07
ZAP 100°C	3.2484	5.2053	1.6024	27.14

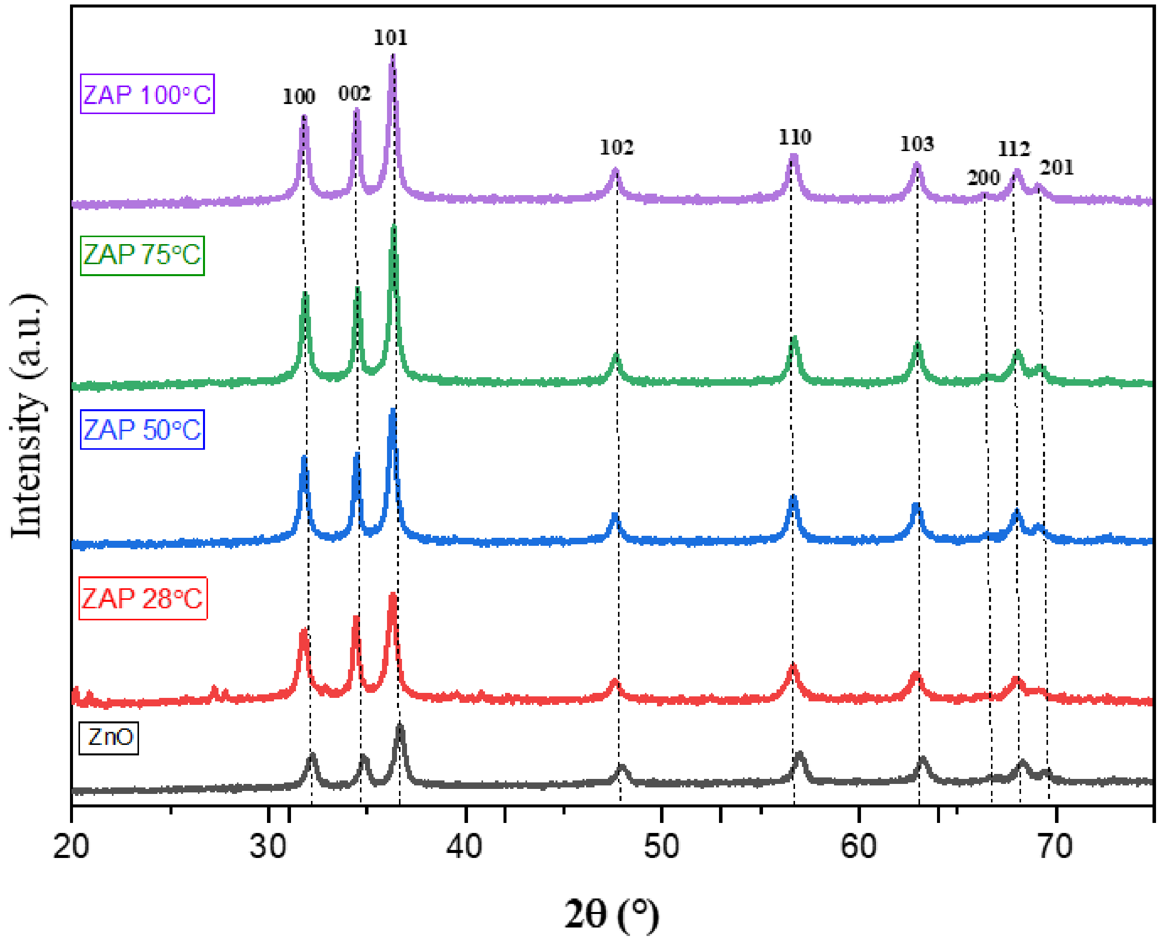

Figure 1. XRD pattern of ZnO and ZAP nanomaterials.

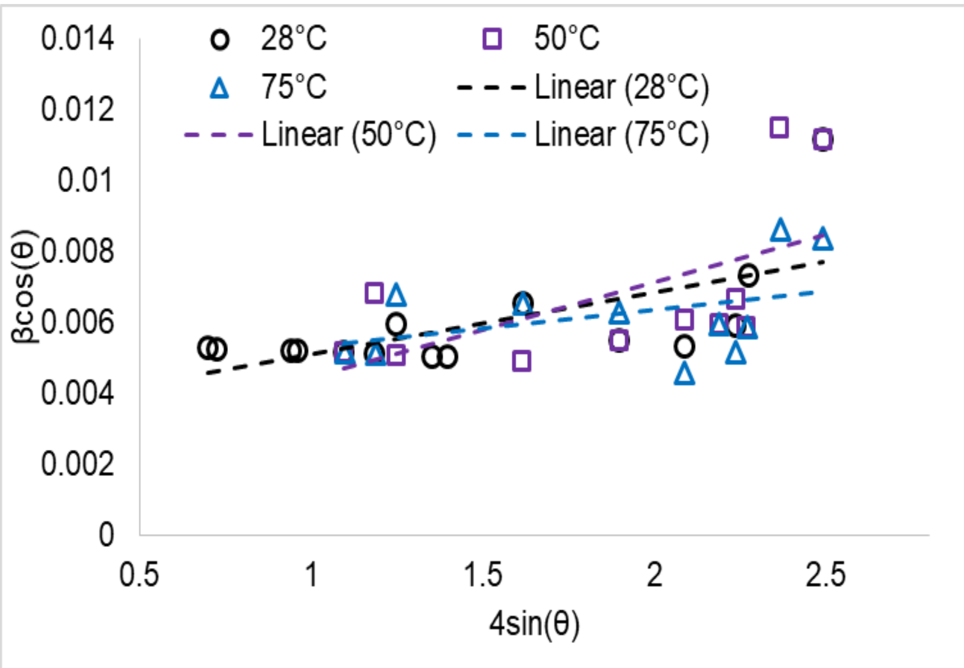

Figure 2. Williamson–Hall plot for the ZAP XRD pattern.

Table 2. Micro-strain analysis of ZAP samples.

Sample	Micro-strain, ε (%)	Equation
ZAP 28°C	0.18	y = 0.0018x + 0.0033
ZAP 50°C	0.27	y = 0.0027x + 0.0017
ZAP 75°C	0.11	y = 0.0011x + 0.0042

Micro-strain analysis from XRD data can be obtained from the Williamson-Hall (WH) plot[27,28]. The observed micro-strain indicates lattice defects in the nanomaterial, which may arise from oxygen vacancies, rapid crystal growth, or low-temperature synthesis conditions[27]. Figure 2 shows the WH plots of the ZAP samples. The slope of the linear fitting plot corresponds to the micro-strain. All ZAP samples show moderate strain, which is likely contributed by rapid-growth effects or low-temperature synthesis.

3.2. Analysis of UV-Vis Spectroscopy

Figure 3 displays the UV-Vis absorbance spectra of the ZnO and ZAP nanoparticles. The UV-Vis spectrum exhibits substantial absorption within the wavelength range of 300-364 nm, as indicated by the characterization results. The ZnO nanomaterials synthesized using pineapple precursors exhibit a spectral profile consistent with ZnO nanoparticles, specifically with wavelengths below 400 nm, as reported by Kumar et al[29]. Figure 3 illustrates the spectral distribution of ZAP at a temperature of 75°C, exhibiting two distinct peaks at wavelengths of 334 nm and 364 nm. As expected, the absorption of ZnO nanomaterials occurs near 364 nm[30,31], whereas the absorption of the plant extract appears around 334 nm. These results indicate that the synthesized sample corresponds to ZnO, which can be verified from the UV-Vis spectral profile and the position of the absorption peaks. The absorption band of ZnO nanoparticles typically falls within the range of 250-400 nm, and the peak observed at 364 nm aligns well with the characteristic optical properties of ZnO.

The UV-Vis spectroscopy technique is commonly employed to determine the band-gap energy value of a sample[32]. The band gap refers to the magnitude of the separation between the valence band and the conduction band in terms of energy levels[33].. Determination of the band gap is accomplished using the Tauc plot approach, as described in the study conducted by Johannes et al. [32]. This method involves graphing the curve of (ahυ2) against the photon energy (hυ). The band-gap energy values acquired for the ZnO and ZAP samples were 3.15 eV, 3.09 eV, 3.07 eV, 3.19 eV, and 3.09 eV, respectively. The disparity in the energy band gap arises from variations in the dimensions of the particles that are produced.

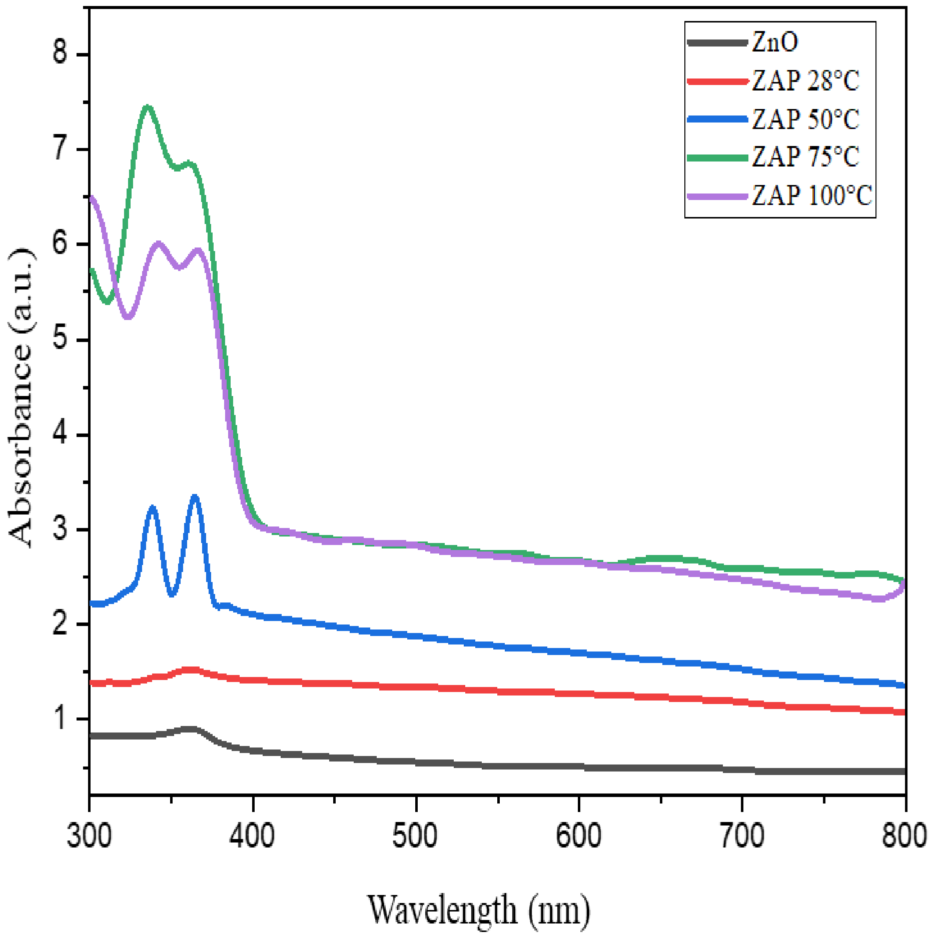

Figure 3. UV-Vis absorption spectra of ZnO and ZAP nanomaterials.

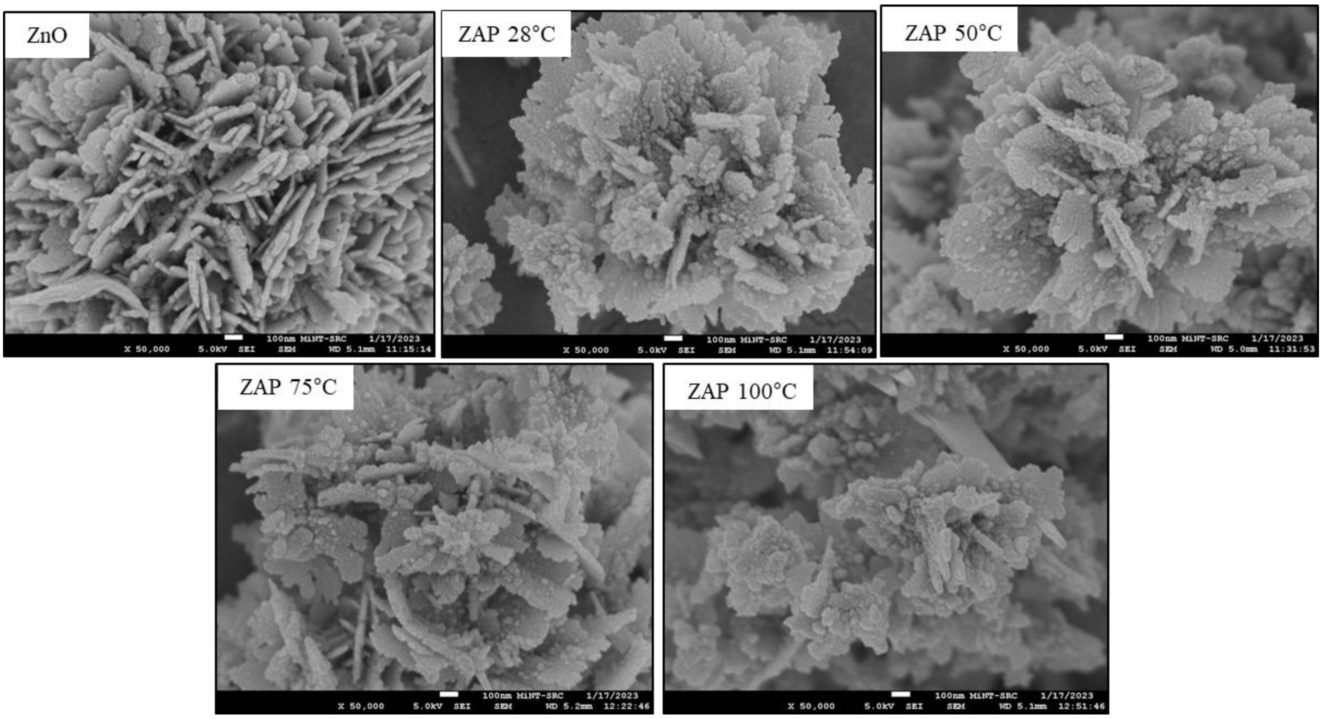

Figure 4. FESEM image of ZnO and ZAP nanomaterials.

3.3. FESEM Analysis

Figure 4 presents an FESEM image of the surface morphology of the ZnO sample at a magnification of 50,000 times. The structural analysis of the ZnO nanomaterial powder reveals that the specimen exhibits a nanoflake morphology, which is characterized by a rough and uneven surface resembling nano-chips. The nanostructure exhibits the occurrence of lumps or agglomeration. The findings presented here align with the prior research conducted by Arasu et al.[34].

The materials known as ZAP 28°C and ZAP 50°C have a hexagonal cross-sectional morphology characterized by sheet-like structures that include slight tapering and irregular surface texture[35]. The findings of this investigation indicate that ZAP 75°C yields the most favorable outcome because of its hexagonal cross-sectional geometry. However, it is worth noting that the inter-particle groups exhibit a higher degree of agglomeration, resulting in the production of smaller materials within larger clusters[36]. . This occurrence can be attributed to the production of ZAP nanoparticles, whereby pineapple fruit extracts are included as reducing agents. At a temperature of 100°C, the sample structure exhibits progressive and pronounced agglomeration[37]. Das et al. [38] showed that the introduction of temperature to the sample affects the arrangement and dispersion of ZnO and ZAP nanoparticles.

3.4. Antibacterial activity test

The disc diffusion method was used to evaluate the antibacterial activity of the synthesized samples. In this study, five discs were prepared: one control disc containing only distilled water and four test discs containing ZAP synthesized at different temperatures (25°C, 50°C, 75°C, and 100°C). E. coli ATCC 25922 was selected because of its clinical relevance and its common use in antibacterial activity assays[39–41].

The first test used chloramphenicol antibiotic as the positive control and distilled water as the negative control, along with the sample. The positive control produced an inhibition zone, indicating the antibiotic’s effect on E. coli bacteria. Meanwhile, the distilled water showed no inhibition zone, indicating the absence of antibacterial activity. This proves that distilled water has no effect on bacterial growth. However, the inhibition zone formed by the antibiotic was larger than that of the sample. This indicates that the ZnO nanomaterial was only able to inhibit the growth of E. coli bacteria on a small scale. The results of the first test are shown in Figure 5.

Figure 6 presents a representative example of the disc diffusion test, in which only two discs are shown for visualization purposes; however, all four ZAP samples and the control disc were tested in the actual experiment. The control disc did not produce any inhibition zone, whereas the four synthesized ZAP samples produced inhibition zones with varying diameters, confirming their antibacterial activity. The diameter of the inhibition zone is directly proportional to the antibacterial strength of a material [42,43].

Among the tested samples, the ZAP synthesized at 75°C produced the largest inhibition zone, as summarized in Table 2. This result indicates that the 75°C ZAP sample exhibited a sharper and more spiky morphology, enabling it to penetrate bacterial cell walls more effectively. The higher permeability of E. coli cell walls to colloidal particles [44] also contributes to the stronger inhibitory effect. The formation of a clear area without bacterial growth indicates a bactericidal effect, in which bacterial growth is suppressed without causing cell lysis[44]. The size of the inhibition zone may vary depending on the bacterial strain, nanoparticle size, and concentration [46]. All four ZAP samples synthesized at different temperatures were included in the antibacterial activity results and discussed comprehensively[45].

Table 3. Inhibition zone data of commercial ZnO and ZAP with temperature variation

Component	Inhibition zone (mm^2)	The ratio to commercial ZnO (%)
Commercial ZnO	1.11	0
ZnO	8.03	623.4
ZAP 28°C	4.71	324.3
ZAP 50°C	4.15	273.9
ZAP 75°C	8.54	669.3
ZAP 100°C	1.43	28.8

Note: the diameter of the inhibition zone including the diameter of the paper disc (6mm).

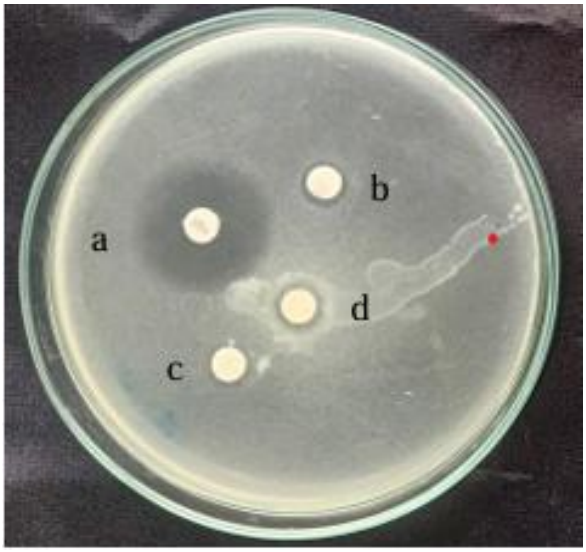

Figure 5. (a) Chloramphenicol antibiotic, (b) 75ºC sample,(c) distilled water, (d) pure pineapple extract.

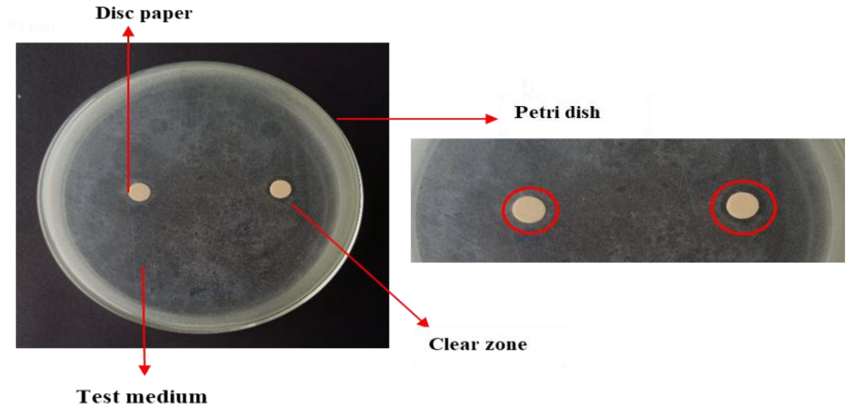

Figure 5. Results test for antibacterial activity of *E. coli*.

4. CONCLUSION

The biosynthesis of ZnO nanoparticles utilizing pineapple extract as a bioreductor, together with subsequent characterization, was successfully accomplished. The use of pineapple fruit extract as a reducing agent and temperature variations throughout the synthesis process affected the crystalline structure, absorption spectra, and morphology of the samples. The mean size of the resultant crystals was 25.84 nm. The utilization of pineapple extract as a bioreducing agent in the manufacture of ZnO nanoparticles resulted in notable inhibition of Escherichia coli bacterial growth, with an observed inhibition-zone diameter of 8.54 mm. The antibacterial activity was enhanced by the formation of a larger inhibition zone.

We acknowledge that elemental analysis of Zn and O was not performed in this study. While the XRD patterns and FESEM results indicate the formation of ZnO, direct confirmation of elemental composition is unavailable. This limitation has been noted, and we recommend that future work include EDX or XPS analyses to quantitatively verify the presence of Zn and O.

Regarding the reviewer's inquiry on the reduction process and functional group identification, the biosynthesis is presumed to be driven by phytochemicals in pineapple extract that typically act as bioreducing agents. However, no functional group analysis (such as FTIR) was conducted to validate this mechanism. This limitation has also been acknowledged, and we suggest that future studies incorporate FTIR or related spectroscopic methods to confirm the functional groups involved in the reduction and stabilization of ZnO nanoparticles.

ACKNOWLEDGMENTS

The authors thank the Institute for Research and Community Service (LPPM), Universitas Riau, for funding this work under the DIPA scheme (Grant No. 8245/UN19.5.1.3/AL.04/2023).

REFERENCES

[1] Kumar P. Nanomaterials synthesis, types and their use in Bioremediation and Agriculture. Natural Resources for Human Health 2022;2:349–65.

[2] Salem SS, Hammad EN, Mohamed AA, El-Dougdoug W. A Comprehensive Review of Nanomaterials: Types, Synthesis, Characterization, and Applications. Biointerface Research in Applied Chemistry 2022;13:41. https://doi.org/10.33263/BRIAC131.041.

[3] Yan Z, Wang X, Yuan D, Xu M, Wang J, Ge H, et al. Antibacterial effect of electrolysis combined with ZnO nanoparticles treatment on heterotrophic bacteria in simulated water. J Environ Chem Eng 2025;13:119110. https://doi.org/10.1016/J.JECE.2025.119110.

[4] Ghodake VS, Koyale PA, Patil SS, Patil PS, Delekar SD. Exploring the antibacterial properties of ZnO nanorods–CuO nanoflowers: a mode of action approach. RSC Adv 2025;15:32995–3005. https://doi.org/10.1039/D5RA04095G.

[5] Maity DrD, Tade R, Sabnis A. Organically modified ZnO nanoparticles incorporated emulsion paints for antibacterial activity. Surfaces and Interfaces 2025;75:107803. https://doi.org/10.1016/J.SURFIN.2025.107803.

[6] Hoye RLZ, Musselman KP, MacManus-Driscoll JL. Research Update: Doping ZnO and TiO2 for solar cells. APL Materials 2013;1:060701. https://doi.org/10.1063/1.4833475.

[7] Ahammed KR, Ashaduzzaman Md, Paul SC, Nath MR, Bhowmik S, Saha O, et al. Microwave assisted synthesis of zinc oxide (ZnO) nanoparticles in a noble approach: utilization for antibacterial and photocatalytic activity. SN Appl Sci 2020;2:955. https://doi.org/10.1007/s42452-020-2762-8.

[8] Shamim A, Mahmood T, Abid M. Biogenic Synthesis of Zinc Oxide (ZnO) Nanoparticles Using a Fungus (Aspargillus niger) and Their Characterization. Int J Chem 2019;11:119. https://doi.org/10.5539/ijc.v11n2p119.

[9] Zhou L, Wang P, Sun T, Chen Y, Cai M, Zheng W, et al. Al2O3 modification of TeO2-ZnO-Na2O glasses: Tailored network structure for enhanced thermal stability and 2–3 μm mid-infrared emission. Opt Laser Technol 2025;190:113244. https://doi.org/10.1016/J.OPTLASTEC.2025.113244.

[10] Chen Y, Bagnall D, Yao T. ZnO as a novel photonic material for the UV region. Materials Science and Engineering: B 2000;75:190–8. https://doi.org/10.1016/S0921-5107(00)00372-X.

[11] Sportelli MC, Gaudiuso C, Volpe A, Izzi M, Picca RA, Ancona A, et al. Biogenic Synthesis of ZnO Nanoparticles and Their Application as Bioactive Agents: A Critical Overview. Reactions 2022;3:423–41. https://doi.org/10.3390/reactions3030030.

[12] Elumalai K, Velmurugan S. Green synthesis, characterization and antimicrobial activities of zinc oxide nanoparticles from the leaf extract of Azadirachta indica (L.). Applied Surface Science 2015;345:329–36. https://doi.org/10.1016/j.apsusc.2015.03.176.

[13] Donia DT, Bauer EM, Missori M, Roselli L, Cecchetti D, Tagliatesta P, et al. Room Temperature Syntheses of ZnO and Their Structures. Symmetry 2021;13:733. https://doi.org/10.3390/sym13040733.

[14] Hassan Basri H, Talib RA, Sukor R, Othman SH, Ariffin H. Effect of Synthesis Temperature on the Size of ZnO Nanoparticles Derived from Pineapple Peel Extract and Antibacterial Activity of ZnO–Starch Nanocomposite Films. Nanomaterials 2020;10:1061. https://doi.org/10.3390/nano10061061.

[15] Liu H, Zhang H, Wang J, Wei J. Effect of temperature on the size of biosynthesized silver nanoparticle: Deep insight into microscopic kinetics analysis. Arabian Journal of Chemistry 2020;13:1011–9. https://doi.org/10.1016/J.ARABJC.2017.09.004.

[16] Machado M de M, Savi BM, Perucchi MB, Benedetti A, Oliveira LFS, Bernardin AM. Effect of Temperature, Precursor Type and Dripping Time on the Crystallite Size of Nano ZnO Obtained by One-Pot Synthesis: 2 *k* Full Factorial Design Analysis. Journal of Nanoscience and Nanotechnology 2018;18:4409–12. https://doi.org/10.1166/jnn.2018.15043.

[17] Iwantono I, Nurwidya W, Lestari LR, Naumar FY, Nafisah S, Umar AA, et al. Effect of growth temperature and time on the ZnO film properties and the performance of dye-sensitized solar cell (DSSC). Journal of Solid State Electrochemistry 2015;19:1217–21. https://doi.org/10.1007/s10008-014-2737-z.

[18] Albaihaqi Y, Abdi R, Natalia S, Syahputra RF, Awitdrus, Iwantono. Palladium role in growth of zno nanostructure with plasmonics layering by seed mediated hydrothermal method. vol. 860 KEM. 2020. https://doi.org/10.4028/www.scientific.net/KEM.860.253.

[19] Uysal Y, Doğaroğlu ZG. Citrus Peel–Mediated ZnO Nanoparticles: Green synthesis, plant responses, and antibacterial activity. Biocatal Agric Biotechnol 2025;70:103854. https://doi.org/10.1016/J.BCAB.2025.103854.

[20] Katiyar A, Kumar N, Srivastava A. Optical properties of ZnO nanoparticles synthesized by co-precipitation method using LiOH. Mater Today Proc

2018;5:9144–7. https://doi.org/10.1016/j.matpr.2017.10.034.

[21] Joshi V, Bachhar V, Mishra SS, Shukla RK, Duseja M. Hexagonal ZnO nanoparticles synthesised using methanolic extract of Piper chaba aerial parts for catalytic oxidation of morin, 4-nitrophenol reduction, antioxidant and antibacterial applications. J Mol Struct 2025;1348:143550. https://doi.org/10.1016/J.MOLSTRUC.2025.143550.

[22] Yang Z, Cao B, Cao Y, An X, Yue X, Guan G, et al. Ultra-sensitive hexagonal wurtzite zinc oxide-based electrochemical sensor for specific recognition of environmental trace N-(1,3-dimethylbutyl)-N′-phenyl-p-phenylenediamine. J Clean Prod 2024;434:140039. https://doi.org/10.1016/J.JCLEPRO.2023.140039.

[23] Wasly H. X-Ray Analysis for Determination the Crystallite Size and Lattice Strain in ZnO Nanoparticles. Journal of Al-Azhar University Engineering Sector 2018;13:1312–20. https://doi.org/10.21608/auej.2018.18943.

[24] Abdulrahman NA. Braggs, Scherre, Williamson–Hall and SSP Analyses to Estimate the Variation of Crystallites Sizes and Lattice Constants for ZnO Nanoparticles Synthesized at different Temperatures. NeuroQuantology 2020;18:53–63. https://doi.org/10.14704/nq.2020.18.1.NQ20107.

[25] Sugihartono I, Silmina AD, Fahdiran R, Isnaeni I. The effects of substrate on enhancement of UV emission of ZnO nanorods. Journal of Physics: Conference Series 2019;1402:066008. https://doi.org/10.1088/1742-6596/1402/6/066008.

[26] Wang Y, Tang W, Zhang L. Crystalline Size Effects on Texture Coefficient, Electrical and Optical Properties of Sputter-deposited Ga-doped ZnO Thin Films. Journal of Materials Science & Technology 2015;31:175–81. https://doi.org/10.1016/j.jmst.2014.11.009.

[27] Lobanov M V., Pomakhina EB, Rebrov AI, Krasovskiy AL, Yaroslavov AA, Shashkeev KA, et al. ZnO Nanoparticle Functionalization by Organosilanes Catalyzed with Ethylene Diamine for Production of Stable Nanodispersions in Water. Russian Journal of Applied Chemistry 2018;91:40–8. https://doi.org/10.1134/S1070427218010068.

[28] Das Bakshi S, Sinha D, Ghosh Chowdhury S. Anisotropic broadening of XRD peaks of α′-Fe: Williamson-Hall and Warren-Averbach analysis using full width at half maximum (FWHM) and integral breadth (IB). Mater Charact 2018;142:144–53. https://doi.org/10.1016/J.MATCHAR.2018.05.018.

[29] Kumar V, Gupta R, Bansal A. Hydrothermal Growth of ZnO Nanorods for Use in Dye-Sensitized Solar Cells. ACS Appl Nano Mater 2021;4:6212–22. https://doi.org/10.1021/acsanm.1c01012.

[30] Chang Q, Xu J, Han Y, Ehrmann A, He T, Zheng R. Photoelectric Performance Optimization of Dye-Sensitized Solar Cells Based on ZnO-TiO2Composite Nanofibers. J Nanomater 2022;2022. https://doi.org/10.1155/2022/7356943.

[31] Vargas MA, Rivera-Muñoz EM, Diosa JE, Mosquera EE, Rodríguez-Páez JE. Nanoparticles of ZnO and Mg-doped ZnO: Synthesis, characterization and efficient removal of methyl orange (MO) from aqueous solution. Ceram Int 2021;47:15668–81. https://doi.org/10.1016/J.CERAMINT.2021.02.137.

[32] Johannes AZ, Pingak RK, Bukit M. Tauc Plot Software: Calculating energy gap values of organic materials based on Ultraviolet-Visible absorbance spectrum. IOP Conf Ser Mater Sci Eng 2020;823:012030. https://doi.org/10.1088/1757-899X/823/1/012030.

[33] Alharshan GA, Aboraia AM, Uosif MAM, Sharaf IM, Shaaban ER, Saad M, et al. Optical Band Gap Tuning, DFT Understandings, and Photocatalysis Performance of ZnO Nanoparticle-Doped Fe Compounds. Materials 2023;16. https://doi.org/10.3390/ma16072676.

[34] Arasu MV, Madankumar A, Theerthagiri J, Salla S, Prabu S, Kim H-S, et al. Synthesis and characterization of ZnO nanoflakes anchored carbon nanoplates for antioxidant and anticancer activity in MCF7 cell lines. Materials Science and Engineering: C 2019;102:536–40. https://doi.org/10.1016/j.msec.2019.04.068.

[35] Dejene BK. Biosynthesized ZnO nanoparticle-functionalized fabrics for antibacterial and biocompatibility evaluations in medical applications: A critical review. Mater Today Chem 2024;42:102421. https://doi.org/10.1016/J.MTCHEM.2024.102421.

[36] Iwantono I, Morsin M, Syajali H, Yudani AF, Ziliwu F, Nafisah S, et al. The performance of plasmonic sensor using gold nanobipyramids and Cu-modified gold nanobipyramids for sensing malathion in Ipomoea aquatica. Advances in Natural Sciences: Nanoscience and Nanotechnology 2025;16. https://doi.org/10.1088/2043-6262/addcde.

[37] Reddy AJ, Kokila MK, Nagabhushana H, Chakradhar RPS, Shivakumara C, Rao JL, et al. Structural, optical and EPR studies on ZnO:Cu nanopowders prepared via low temperature solution combustion synthesis. Journal of Alloys and Compounds 2011;509:5349–55. https://doi.org/10.1016/j.jallcom.2011.02.043.

[38] Das C, Sen S, Singh T, Ghosh T, Paul SS, Kim TW, et al. Green Synthesis, Characterization and Application of Natural Product Coated Magnetite Nanoparticles for Wastewater Treatment. Nanomaterials 2020;10:1615. https://doi.org/10.3390/nano10081615.

[39] Abbas A. Antibacterial Activities of Various Antibiotics Against Clinical Isolates of Escherichia coli. Pakistan BioMedical Journal 2022:40–3. https://doi.org/10.54393/pbmj.v5i10.841.

[40] Hannah S, Dobrea A, Lasserre P, Blair EO, Alcorn D, Hoskisson PA, et al. Development of a Rapid, Antimicrobial Susceptibility Test for E. coli Based on Low-Cost, Screen-Printed Electrodes. Biosensors 2020;10:153. https://doi.org/10.3390/bios10110153.

[41] Morozov A, Mgebrishvili S, Dorenskaya A, Aleksanyan K, Salmanova K, Sorokovikova T, et al. Antibiotic Resistance of E. Coli in Clinical Practice. Archiv Euromedica 2022;12. https://doi.org/10.35630/2022/12/6.12.

[42] Naqvi Q-A, Kanwal A, Qaseem S, Naeem M, Ali SR, Shaffique M, et al. Size-dependent inhibition of bacterial growth by chemically engineered spherical ZnO nanoparticles. Journal of Biological Physics 2019;45:147–59. https://doi.org/10.1007/s10867-019-9520-4.

[43] Ahmad RAR, Harun Z, Othman MHD, Basri H, Yunos MZ, Ahmad A, et al. Biosynthesis of zinc oxide nanoparticles by using fruits extracts of Ananas Comosus and its antibacterial activity. Malaysian Journal of Fundamental and Applied Sciences 2019;15:268–73. https://doi.org/10.11113/mjfas.v15n2.1217.

[44] Raffi M, Mehrwan S, Bhatti TM, Akhter JI, Hameed A, Yawar W, et al. Investigations into the antibacterial behavior of copper nanoparticles against Escherichia coli. Annals of Microbiology 2010;60:75–80. https://doi.org/10.1007/s13213-010-0015-6.

[45] Karvani ZE, Chehrazi P. Antibacterial activity of ZnO nanoparticle on Gram-positive and Gram-negative bacteria. African Journal of Microbiology Research 2012;5:1368–73. https://doi.org/10.5897/AJMR10.159.